DOI: 10.1002/cphc.201300162

Printable Magnetoelectronics

Denys Makarov,*[a] Daniil Karnaushenko,[a, b] and Oliver G. Schmidt[a, b, c]

The field of printable electronics is well developed. A large variety of electronic components assembled as printable optoelectronic devices and communication modules are already available. However, the element responding to a magnetic field, which is highly demanded for the concept of printable electronics has only been realized very recently. A printable magnetic sensing device has been one of the remaining missing building blocks crucial to realize the concept of entirely printable electronics. Here, we position the novel topic of printable magnetic sensorics in a family of printable electronics and highlight possible application directions of this technology.

1. Introduction

Printed electronics are about to revolutionize the field of conventional electronics offering low-cost, large-area, high-volume, high-throughput production in roll-to-roll or sheet-feed processing techniques. Electronic components fabricated by printing are light-weight and small, thin and flexible, inexpensive and disposable.[1,2] Cost advantages of more than 10 times per unit area compared to conventional lithography-based fabrication appear quite feasible.[3] Already at the very beginning of the development of this technological platform various applications directions for printed electronics aiming for transparent, bendable/flexible functional devices have been proposed (Figure 1): displays,[4,5] including organic light-emitting diodes (OLEDs),[6,7] liquid crystal displays (LCDs),[8] various types of sensors,[9–12] radio-frequency identification (RFID) tags[13–17] and organic solar cells.[18–20] Leading printed electronics companies like Heraeus, PolyIC, Plastic Logic and Printechnologics presented fascinated innovations in several application areas:[21]

- Lighting (OLED)
- Electronic components (printed RFIDs, memories, batteries)
- Organic photovoltaics
- Displays
- Intelligent systems (Integrated Smart Systems, sensors).

Flexible displays based on organic light-emitting diodes (OLEDs), organic solar cells, printed batteries, glucose tests sensors and e-Ink (electronic ink) are already on the market. Printed data memories and RFID chips are currently making the transition to industrial production.[21] In addition to the cost efficiency of printed electronic devices, the printing approach allows a reduction in the overall process complexity. Indeed, in contrast to lithography + etch-based subtractive processing of conventional microelectronics, printable platforms open the way towards entirely additive processing. This is a tremendous advantage, since it reduces overall step count, raw material costs, and overall tooling cost, therefore reducing capital expenditure and increasing throughput across the entire flow.[3]

To realize printable electronics, it is necessary to develop inks or pastes that can be printed that will result in inductors, capacitors, batteries, interconnects, resistors, transistor, diodes, memories, and sensing and display elements. Four conventional mass-printing techniques exist, named after the type of master used for printing: relief printing (flexographic), intaglio printing (gravure), planographic printing (offset), and print through (screen printing).[2,22] Depending on the specific requirements of the fabrication process, like temperature, viscosity of the ink, substrate material careful choice of the printing method has to be made. For instance, inkjet printing allows the printing of different semiconductor inks on the same substrate, thus allowing for the realization of arrays of different transistors in a very economical and efficient manner.

With respect to the recently developed printable magnetoelectronics,[12] the most suitable printing technology seems to be screen printing. Screen printing is a well-established technique for fabrication of printed conductor traces[23] (typically using silver pastes), resistors (using carbon films), capacitors (using polyimide dielectrics), for printed circuit boards. In screen printing,[24] ink is pressed with a squeegee through a screen onto the substrate. The screen is typically made of a mesh. Due to the simplicity of the process, a wide variety of

[a] Dr. D. Makarov, D. Karnaushenko, Prof. Dr. O. G. Schmidt
Institute for Integrative Nanosciences
Leibniz Institute for Solid State and
Materials Research Dresden (IFW Dresden)
Helmholtzstr. 20, 01069 Dresden (Germany)
Fax: (+49) 351 4659 648
E-mail: d.makarov@ifw-dresden.de

[b] D. Karnaushenko, Prof. Dr. O. G. Schmidt
Material Systems for Nanoelectronics
Chemnitz University of Technology
Reichenhainer Strasse 70, 09107 Chemnitz (Germany)

[c] Prof. Dr. O. G. Schmidt
Merge Technologies for Multifunctional Lightweight Structures
Chemnitz University of Technology
Reichenhainer Strasse 70, 09107 Chemnitz (Germany)

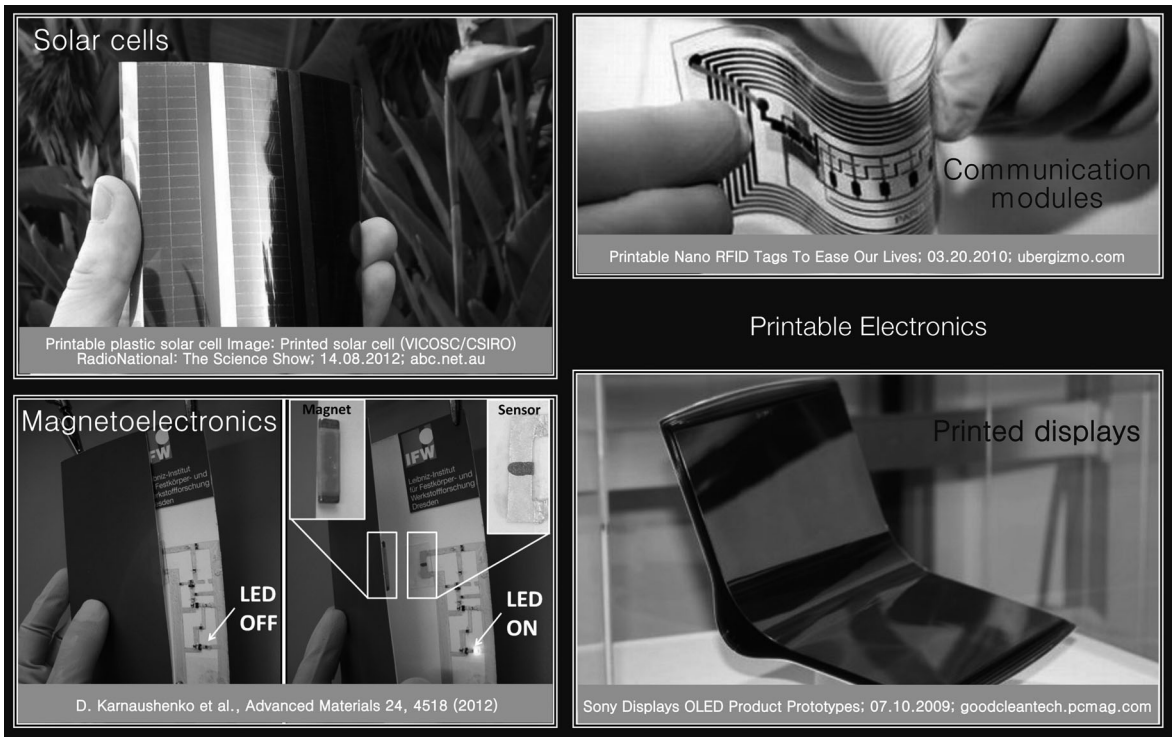

Figure 1. The family of printable electronic devices includes solar cells, printable displays and communication modules. Recently, a new member has been added to the family, namely printable magnetoresistive sensor elements.

substrates and inks can be used, allowing a high layer thickness, which is typical for screen printing. In industrial processes, screen-printed films usually have a thickness larger than about 0.5 μm.[25,26] Silk screen-printed polymer solar cells have been reported on polyethylene terephthalate (PET) foil by Krebs et al.[27] Flexible pentacene transistors,[28] complementary metal oxide semiconductor (CMOS) devices on polyethylene naphthalate (PEN) foil[29] as well as flexible thin film supercapacitors on polyester (PE) foils realized using screen printing have been reported.[30]

1.1. Printable Magnetoelectronics

In order to realize the vision of printable electronics, it is necessary to replicate all components of conventional rigid electronics in a printable form. The field of modern electronics is very general, including interconnects, optoelectronics and magnetoelectronics. Although cost-efficient versatile electronic building blocks, such as transistors, diodes and resistors, resulting in printable optoelectronics and printable communication modules are already available as printed counterparts of conventional semiconductor elements, printable magnetoelectronics and contactless magnetic field driven switches operating at ambient conditions had been reported only very recently.[12] For this purpose, magnetic sensors with high sensitivity operating at room temperature have to be developed as inks, pastes or paints. The fabrication of printable magnetoelectronics is challenging, mainly due to the lack of appropriate sensing compounds at ambient conditions. In order to be in line with the concept of printable electronics, magnetic sensors should satisfy the following basic requirements: low-cost, high-volume production on large areas of standard printing materials, disposability and processability.

In this respect, it is known that magnetic nanoparticles surrounded by a non-magnetic matrix reveal various spin-dependent transport phenomena.[31–36] Thus, they may act as magnetoresistive sensor devices potentially enabling the realization of printable magnetoresistive sensorics. First, the giant magnetoresistive (GMR) effect in granular Co/Cu systems was reported in 1992 by Xiao et al.[37] and Berkowitz et al.[38] Typically, granular materials are prepared by top-down methods such as sputtering as well as by metallurgic techniques.[39–43] However, it was suggested that bottom-up chemical syntheses for nanoparticle fabrication offer significant advantages:[44–46] using ligands with different chain lengths allows to tune the particle–matrix volume fraction and the interparticle distances between the magnetic granules.[47] A first bottom-up approach for the preparation of granular structures is based on the simultaneous deposition of particles, which are prefabricated in the gas phase, and the matrix material on a cold surface.[44]

Depending on the material of the interparticle matrix, different effects may occur: insulating material result in tunnelling magnetoresistance (TMR), the use of conducting matrices in giant magnetoresistance (GMR) effects.

1.2. Tunnelling Magnetoresistive Sensors

The focus here is on assemblies of pure metallic nonoxidized magnetic nanoparticles (MNPs) made of Co, Fe, Ni, or their alloys and stabilized by an organic shell. The stabilizing organic

ligands surrounding the MNPs are expected to act as a tunnel barrier.[48] Hybrid systems where the particles were embedded in organic semiconductors such as fullerene C_{60},[49] rubrene[50] or Alq_3[51] exhibited MR values in the range of up to 100% at low temperatures. An important issue is whether the organic ligands surrounding the magnetic particles could be an efficient tunnel barrier up to room temperature. Tan et al. showed that chemically synthesized, ligand-stabilized nanoparticles can be used for a bottom-up preparation of granular TMR systems.[34,35] TMR amplitudes of up to 3000% at low temperatures have been reported in such granular three-dimensional self-assembled supercrystals consisting of FeCo nanoparticles. At the moment, in the best cases MR always decreased down to 0.1% at room temperature.[49–51] This strong decay of magnetoresistance as a function of temperature is attributed to a spin-flip process enhanced by transferred charges at localized states within the organic barrier.

Only recently, the room-temperature TMR was observed in assemblies of fully metallic iron MNPs synthesized by organometallic chemistry.[52] Figure 2 displays the magnetic field dependence of the magnetic-field-dependent resistivity $R(H)$ for a sample with cubic Fe nanoparticles with a mean size of 8.9 nm surrounded by hexadecylamine $[CH_3(CH_2)_{15}NH_2]$/hexadecylammonium $[CH_3(CH_2)_{15}NH_3^+Cl^-]$. The measurable resistances of the devices ranged from 5 to 6 MΩ at room temperature. The magnetoresistance curves evidence two contributions. At a high magnetic field, the first one is characterized by a linear decrease of R. The associated MR is weakly dependent on temperature. The second contribution occurs at a low applied magnetic field <0.5 T and persists up to high temperatures. This was attributed to the spin-dependent tunnelling between the NPs. In Figure 2d, the temperature evolution of the TMR is shown. The amplitude of TMR is 0.9% and 0.3% at $T=2$ K and $T=300$ K, respectively. Demonstration of the TMR at room temperature in assemblies of magnetic nanoparticles is the first important step towards their application for printable magnetic sensorics. However, the TMR magnitude at room temperature has to be improved further.

1.3. Giant Magnetoresistive Sensors

Weddemann et al.[47] investigated the transport properties in two-dimensional monolayers of Co nanocrystals embedded in a conducting matrix. Therefore, 8 nm Co particle assemblies have been created in a dropping procedure. After the self-assembly process, the insulating ligand shells were removed by heating the particles for about 4 h at 400 °C in a reducing gas atmosphere. Subsequently, a thin Cu layer was deposited on top of the nanocrystals. The magneto-electrical characterization of the samples at room temperature is shown in Figure 3. A GMR amplitude of about 4% was observed. Although a room-temperature GMR response is demonstrated, the resistance of the sample is too large (~100 MΩ) due to the small thickness of the sample, which is inappropriate for applications in printable magnetoelectronics. Furthermore, the orientations of magnetic moments in such 2D assemblies are correlated along domains with an antiparallel orientation similar to ferromagnetic materials. Consequently, the evolution of the magnetic configuration strongly depends on the history of the magnetic pattern and repeated measurements made under identical conditions may result in significantly deviating findings.[47]

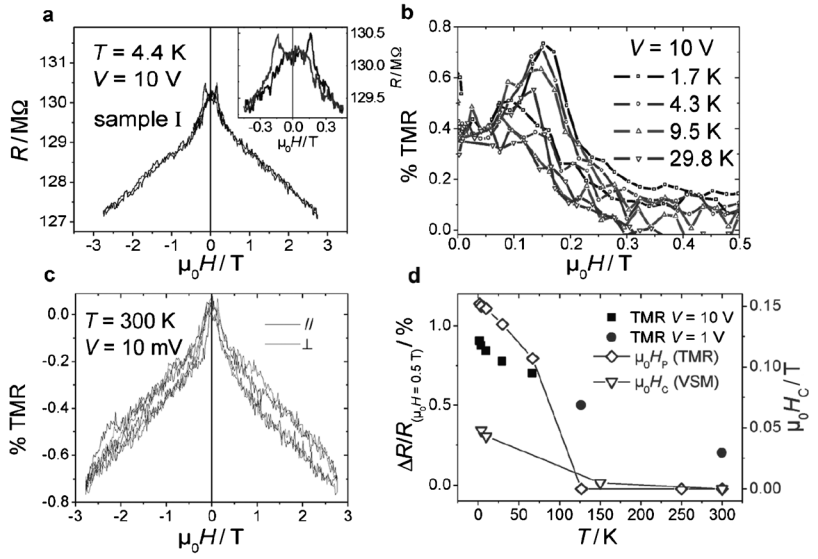

Figure 2. a) Magnetoresistance of Fe nanocubes at $T=4.4$ K. Insert: low-field region. The lines indicate the sweep up and back of the applied magnetic field. b) Temperature dependence of $R(H)$ characteristics for $V=10$ V. c) Magnetoresistance of Fe nanocubes at room temperature with the magnetic field applied in and out of the plane of the device (black and grey lines respectively). d) Temperature dependence of the tunnel magnetoresistance of Fe nanocubes (■, ●), coercive field deduced from the magnetoresistance curves (◇) and from magnetization measurements (▽). Reprinted with permission from J. Dugay, R. P. Tan, A. Meffre, T. Blon, L.-M. Lacroix, J. Carrey, P. F. Fazzini, S. Lachaize, B. Chaudret, M. Respaud, "Room-Temperature Tunnel Magnetoresistance in Self-Assembled Chemically Synthesized Metallic Iron Nanoparticles", *Nano Lett.* **2011**, *11*, 5128–5134. Copyright 2011 American Chemical Society.

2. Results and Discussion

Recently, magneto-sensitive inks revealing a GMR effect at room temperature were developed.[12] in brief, they are fabricated by growing GMR stacks consisting of 50[Co(1.0 nm)/Cu(1.2 nm)] bilayers on top of a polymer buffer layer prepared on a rigid wafer. It was previously demonstrated that the GMR performance does not change for samples prepared on rigid Si wafers or on organic films covering Si wafers.[53–56] After deposition, the samples are rinsed in acetone to release the GMR stacks from the substrates. The metallic film is filtered out, dried and then ball-milled. The resulting powder is filtered through a grid that limits the maximum lateral size of

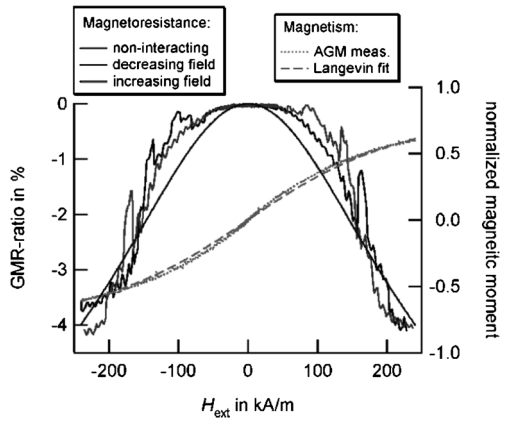

Figure 3. GMR response of a monolayer consisting of 8 nm Co particles covered by a thin Cu film. Measurements were taken at room temperature with a sample current of 1 mA and an in-plane external magnetic field. In comparison to the prediction of non-interacing particles, the experiments show additional features at field values of about $\pm 176\ kA\,m^{-1}$, $\pm 136\ kA\,m^{-1}$ and $\pm 88\ kA\,m^{-1}$. Image is taken from A. Weddemann, I. Ennen, A. Regtmeier, C. Albon, A. Wolff, K. Eckstädt, N. Mill, M. K.-H. Peter, J. Mattay, C. Plattner, N. Sewald, A. Hütten, "Review and outlook: from single nanoparticles to self-assembled monolayers and granular GMR sensors", *Beilstein J. Nanotechnol.* **2010**, *1*, 75–93.

flexibility and good adhesion to standard printing materials. Using a brush the solution was painted on different surfaces, that is, paper, polymers and ceramic (Figure 4b). Due to the relatively large size of the individual GMR flakes, the painted GMR sensors are operational at ambient conditions. The typical thickness of the sensor is in the range of 200 μm.

2.1. Magneto-Electric Characterization

In order to contact the fabricated magnetic sensors electrically, a regular silver paste is used by direct brush painting on the sensor surface. The average conductivity is about $15\ S\,m^{-1}$ for the painted sensors determined by the percolation of the GMR flakes and is independent of the substrate material. The resistance of the sensor varies in a range from 50 to 2000 Ω (Figures 4c,d), which is defined by the painting geometry and ink thickness. This resistance value allows an easy evaluation of the sensor's response without complex amplification electronics. Figures 4c,d show the GMR ratio measured at room temperature for sensors painted on a rigid Si wafer and on a paper. The GMR ratio is defined as the magnetic-field-dependent change in the sample's resistance, $R(H_{ext})$, normalised to the resistance value of the magnetically saturated sample, R_{sat}: $GMR(H_{ext}) = [R(H_{ext}) - R_{sat}]/R_{sat}$. The GMR ratio is averaged within the compound resulting in a linear response at fields of up to 0.7 T. Furthermore, the sensors show only a slight anisotropic response (Figures 4c,d), which allows one to perform measurements in any direction of an applied magnetic field. The almost isotropic response of the painted sensors is caused by the random orientation of the GMR flakes in the binder solution. This isotropy of the sensor is of great advantage, since no special alignments of the magnet are required, while conventional planar GMR sensors are highly anisotropic.

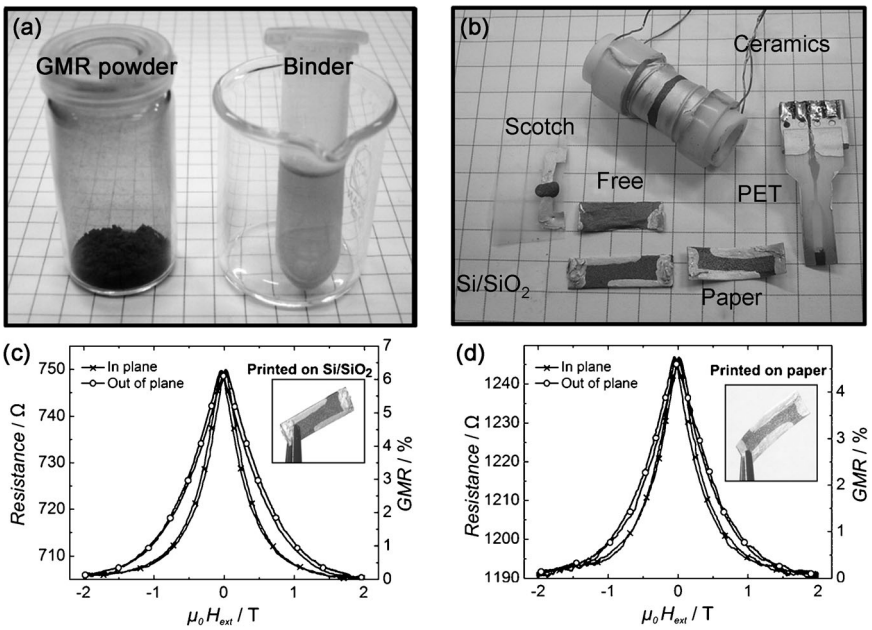

Figure 4. a) Preparation of a GMR paste: GMR powder has to be mixed with a binder solution. b) GMR paste can be painted on various surfaces (curved and planar) of rigid as well as flexible substrates. Magneto-electric characterization of the magnetic GMR sensors painted c) on a rigid SiOx/Si wafer and d) on a paper. Image is adopted from D. Karnaushenko, D. Makarov, C. Yan, R. Streubel, O. G. Schmidt, "Printable Giant Magnetoresistive Devices", *Adv. Mater.* **2012**, *24*, 4518–4522.

2.2. Printed GMR-Based Switch

To demonstrate the functionality of a printable GMR sensor element at a proof-of-concept level, the sensor was integrated in an electronic circuit fabricated directly on the paper of a postcard (Figure 5). Conductive silver paste was used to paint interconnects, which are the main components in modern printed electronics. For demonstration, we chose a hybrid circuit consisting of painted elements (interconnects and sensor) combined with conventional solid state discrete transistors, capacitors, resistors and a light emitting diode (LED). When the postcard is

a GMR flake to about 150 μm. A magneto-sensitive ink is prepared by mixing 500 mg of the GMR powder with 1 mL of a binder solution (Figure 4a).

An acrylic rubber based on poly(methyl methacrylate) (PMMA) that is dissolved in a methyl isobutyl ketone carrier was used as a binder material. The binder prevents oxidation of the GMR powder and fulfils requirements of mechanical

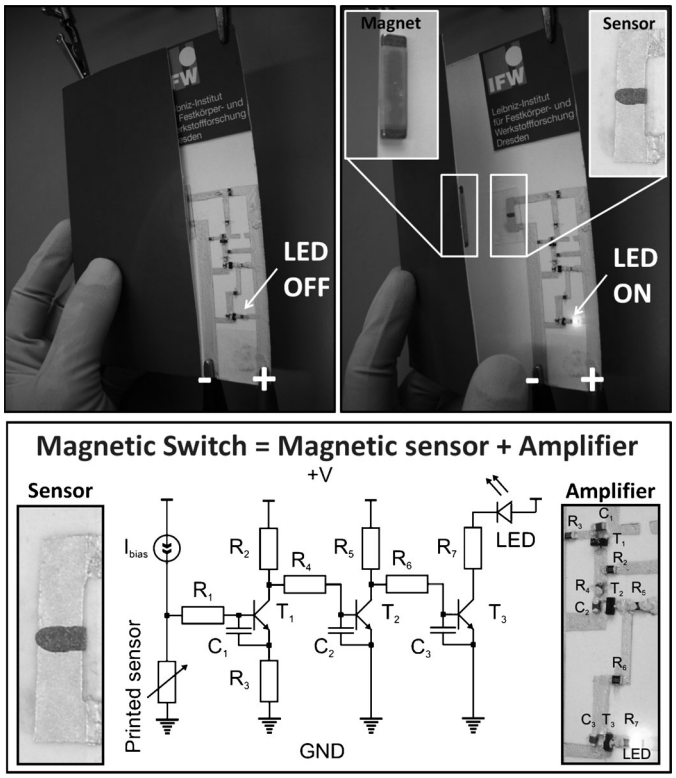

Figure 5. Top: Printable magnetic sensor integrated in a hybrid electronic circuit (amplification cascade with an LED) fabricated on the paper of a postcard. The LED ON/OFF state is triggered by a permanent magnet that modifies the resistance of the sensor. This change in resistance, in turn, alters the open/close state of the transistors in the amplification cascades regulating the current flow through the LED. Bottom: Magnified view of the hybrid electronic circuit with the printed magnetic sensor. The amplification circuit contains current source I_{bias} to bias the sensor, three amplification cascades with three transistors T_1-T_3, resistors R_1–R_7 and capacitors C_1–C . The last amplification cascade supplies LED. Image is adopted from D. Karnaushenko, D. Makarov, C. Yan, R. Streubel, O. G. Schmidt, "Printable Giant Magnetoresistive Devices", *Adv. Mater.* **2012**, *24*, 4518–4522.

closed, the LED is switched off (Figure 5). Opening the postcard switches on the LED. The ON/OFF state of the LED is triggered by a small permanent magnet that modifies the resistance of the printable magnetic sensor. This change in resistance, in turn, alters the open/close state of the transistors in the amplification cascades (Figure 5) regulating the current flow through the LED. Note that all these discrete elements (resistors, transistors, diodes) used for electronic circuitry as well as the permanent magnets are available for printable electronics.[20] Therefore, the fabrication of a fully printable circuit with an integrated magnetic sensor is possible.

3. Conclusions

By adding a magnetic sensor to well-established printable electronics platform, active intelligent packaging, postcards, books or promotional materials that communicate with the environment could be envisioned. The printable magnetic sensor would act as a contactless switch in a complex electronic circuit consisting of, for example, transistors, capacitors and batteries. Combined with RFID tag and printed antenna, integrated functions of the printed electronic circuit like data exchange can be externally triggered by a magnetic field. Our demonstrator with a magnetic switch printed on a postcard suggests that this vision on interactive fully printable electronics can become reality.

There are several issues which have to be solved on the way towards commercialization of this technology. Among them the most crucial are high-volume production of magneto-sensitive ink and demonstration of large-scale printing of the ink. There are strategies that will help us to overcome the aforementioned aspects. To increase the produced amount of the ink it is instructive to choose different support materials. The best would be to switch from the Si-based substrates to large-area polymer sheets. We already demonstrated that magnetic sensors with good GMR response can be prepared even on regular transparency. Regarding the second issue, at the moment, we are applying a regular painting process to bring the magneto-sensitive ink to the surface. Potentially, other methods, such as roll-to-roll, flexography, spray coating and screen printing can be applied. However, the size of the GMR flakes in the ink as well as the viscosity of the ink has to be optimized separately for each of these printing processes. In this respect, more investigations are required to understand the influence of the size of GMR flakes on the resulting GMR response of the magneto-sensitive ink. Furthermore, different binder solutions have to be tested to adjust the viscosity of the ink.

Experimental Section

Preparation of $[Co/Cu]_{50}$ GMR Multilayers

To obtain a large GMR ratio, a Co(1.0 nm)/$[Cu(1.2\ nm)/Co(1.0\ nm)]_{50}$ multilayer stack is deposited at room temperature by means of magnetron sputter deposition with a rate of 2 Å s^{-1} (base pressure: 7.0×10^{-7} mbar, Ar sputter pressure: 7.5×10^{-4} mbar). The thickness of individual Co and Cu layers was optimised in order to achieve Co/Cu multilayers coupled in the first antiferromagnetic maximum. Please note that the GMR stack during preparation is smooth (RMS roughness is about 0.6 nm).[54]

Magneto Electrical Characterisation of the GMR Sensors

An electrical connection between the sensor and a single acquisition board device is realised in a four-point measurement configuration by gluing copper wires to the sensor with silver paint (ACHESON Silver DAG 1415). The response of sensor to an external magnetic field is detected by measuring changes in its resistance. The sensor bias current produced by a constant-current generator circuit, which is implemented directly into acquisition device, is set to 1 mA. Moreover, the magnetic field is measured by a conventional Hall-effect sensor connected to a parallel channel of acquisition device. An electromagnet sweeps the magnetic field with a frequency of 1 Hz parallel or normal to the substrate. The voltage signals of both channels are simultaneously acquired, amplified and adjusted to the input range of an analog-to-digital converter, which is embedded in the microcontroller unit (MCU) of the acquisition device. After processing in MCU the data is sent to a per-

sonal computer by means of a universal serial bus interface at a rate of 2000 measured points per second.

Acknowledgements

The authors acknowledge strong contribution of R. Streubel and Dr. C. Yan (IFW Dresden). Valuable discussions with Dr. J. I. Mönch, T. Kosub and M. Melzer (IFW Dresden) are greatly appreciated. We thank I. Fiering and D. D. Karnaushenko (IFW Dresden) for the support in the fabrication of magnetic multilayers. This work is financed in part by the BMBF project Nanett (federal research funding of Germany FKZ: 03IS2011F), DFG Research Unit 1713 "Sensoric Micro and Nanosystems" and European Research Council under the European Union's Seventh Framework Programme (FP7/2007-2013) / ERC grant agreement n° 306277.

Keywords: giant magnetoresistive effect · magnetic inks · magnetoelectronics · printable electronics · printable sensors

[1] V. Kantola, J. Kulovesi, L. Lahti, R. Lin, M. Zavodchikova, E. Coatanéa in *Bit Bang—Rays to the Future* (Eds.: Y. Neuvo, S. Ylönen), Helsinki University Print, Helsinki, **2009**, pp. 63 – 102.
[2] P. F. Moonen, I. Yakimets, J. Huskens, *Adv. Mater.* **2012**, *24*, 5526 – 5541.
[3] V. Subramanian, J. B. Chang, A. de La Fuente Vornbrock, D. C. Huang, L. Jagannathan, F. Liao, B. Mattis, S. Molesa, D. R. Redinger, D. Soltman, S. K. Volkman, Q. Zhang, Proc. 38th Eur. Solid-State Device Res. Conf. ESSDERC, **2008**.
[4] H. Sirringhaus, N. Tessler, R. H. Friend, *Science* **1998**, *280*, 1741.
[5] J. Jacobson, B. Comiskey, J. D. Albert, H. Yoshizawa, *Nature* **1998**, *394*, 253 – 255.
[6] N. C. van der Vaart, H. Lifka, F. P. M. Budzelaar, J. E. J. M. Rubingh, J. J. L. Hoppenbrouwers, J. F. Dijksman, R. G. F. A. Verbeek, R. Van Woudenberg, F. J. Vossen, M. G. H. Hiddink, J. J. W. M. Rosink, T. N. M. Bernards, A. Giraldo, N. D. Young, D. A. Fish, M. J. Childs, W. A. Steer, D. Lee, D. S. George, *J. Soc. Inf. Disp.* **2005**, *13*, 9.
[7] B. Geffroy, P. le Roy, C. Prat, *Polym. Int.* **2006**, *55*, 572 – 582.
[8] I. Shiyanovskaya, A. Khan, S. Green, G. Magyar, O. Pishnyak, J. W. Doane, *Proc. SPIE-Int. Soc. Opt. Eng.* **2005**, *5801*, 204.
[9] B. Crone, A. Dodabalapur, A. Gelperin, L. Torsi, H. E. Katz, A. J. Lovinger, Z. Bao, *Appl. Phys. Lett.* **2001**, *78*, 2229.
[10] F. Liao, C. Chen, V. Subramanian, *Sens. Actuators B* **2005**, *107*, 849.
[11] T. Someya, T. Sekitani, S. Iba, Y. Kato, H. Kawaguchi, T. Sakurai, *Proc. Natl. Acad. Sci. USA* **2004**, *101*, 9966 – 9970.
[12] D. Karnaushenko, D. Makarov, C. Yan, R. Streubel, O. G. Schmidt, *Adv. Mater.* **2012**, *24*, 4518 – 4522.
[13] W. Clemens, W. Fix, J. Ficker, A. Knobloch, A. Ullmann, *J. Mater. Res.* **2004**, *19*, 1963.
[14] V. Subramanian, P. C. Chang, J. B. Lee, S. E. Molesa, S. K. Volkman, *IEEE Trans. Compon. Packag. Technol.* **2005**, *28*, 742 – 747.
[15] Y. J. Chan, C. P. Kung, Z. Pei, IEEE International Workshop on Radio-Frequency Integration Technology, **2005**, pp. 139 – 141.
[16] S. Steudel, S. De Vusser, K. Myny, M. Lenes, J. Genoe, P. Heremans, *J. Appl. Phys.* **2006**, *99*, 114519.
[17] P. F. Baude, D. A. Ender, M. A. Haase, T. W. Kelley, D. V. Muyres, S. D. Theiss, *Appl. Phys. Lett.* **2003**, *82*, 3964 – 3966.
[18] T. Kietzke, *Adv. Opt. Electron.* **2007**, 40285.
[19] A. Yella, H.-W. Lee, H. N. Tsao, C. Yi, A. Kumar Chandiran, Md. Khaja Nazeeruddin, E. W.-G. Diau, C.-Y. Yeh, S. M. Zakeeruddin, M. Grätzel, *Science* **2011**, *334*, 629.
[20] Y. Sun, G. C. Welch, W. L. Leong, C. J. Takacs, G. C. Bazan, A. J. Heeger, *Nat. Mater.* **2012**, *11*, 44.
[21] review Printed electronics (special topic preview) at www.drupa.com: http://www.drupa.com/cipp/md_drupa/custom/pub/content,oid,26173/lang,2/ticket,g_u_e_s_t/~/review_Printed_Electronics.html.
[22] H. W. Vollmann, *Angew. Chem.* **1980**, *92*, 95 – 106; *Angew. Chem. Int. Ed. Engl.* **1980**, *19*, 99 – 110.
[23] Y. Noguchi, T. Sekitani, T. Someya, *Appl. Phys. Lett.* **2007**, *91*, 133502.
[24] R. Søndergaard, M. Hösel, D. Angmo, T. T. Larsen-Olsen, F. C. Krebs, *Mater. Today* **2012**, *15*, 36 – 49.
[25] S. E. Shaheen, R. Radspinner, N. Peyghambarian, G. E. Jabbour, *Appl. Phys. Lett.* **2001**, *79*, 2996 – 2998.
[26] D. A. Pardo, G. E. Jabbour, N. Peyghambarian, *Adv. Mater.* **2000**, *12*, 1249 – 1252.
[27] F. C. Krebs, J. Alstrup, H. Spanggaard, K. Larsen, E. Kold, *Sol. Energy Mater. Sol. Cells* **2004**, *83*, 293 – 300.
[28] I. E. H. El Jazairi, T. Trigaud, J.-P. Moliton, *Micro Nanosyst.* **2009**, *1*, 46 – 49.
[29] M. Guerin, A. Daami, S. Jacob, E. Bergeret, E. Benevent, P. Pannier, R. Coppard, *IEEE Trans. Electron Devices* **2011**, *58*, 3587 – 3593.
[30] X. Ji, P. M. Hallam, S. M. Houssein, R. Kadara, L. Lang, C. E. Banks, *RSC Adv.* **2012**, *2*, 1508 – 1515.
[31] S. Wang, F. J. Yue, D. Wu, F. M. Zhang, W. Zhong, Y. W. Du, *Appl. Phys. Lett.* **2009**, *94*, 012507.
[32] H. Zeng, C. T. Black, R. L. Sandstrom, P. M. Rice, C. B. Murray, S. Sun, *Phys. Rev. B* **2006**, *73*, 020402(R).
[33] T. Wen, D. Liu, C. K. Luscombe, K. M. Krishnan, *Appl. Phys. Lett.* **2009**, *95*, 082509.
[34] R. P. Tan, J. Carrey, C. Desvaux, J. Grisolia, P. Renaud, B. Chaudret, M. Respaud, *Phys. Rev. Lett.* **2007**, *99*, 176805.
[35] R. P. Tan, J. Carrey, M. Respaud, C. Desvaux, P. Renaud, B. Chaudret, *J. Magn. Magn. Mater.* **2008**, *320*, L55 – L59.
[36] S. S. P. Parkin, *Annu. Rev. Mater. Sci.* **1995**, *25*, 357.
[37] J. Q. Xiao, J. S. Jiang, C. L. Chien, *Phys. Rev. Lett.* **1992**, *68*, 3749 – 3752.
[38] A. E. Berkowitz, J. R. Mitchell, M. J. Carey, A. P. Young, S. Zhang, F. E. Spada, F. T. Parker, A. Hütten, G. Thomas, *Phys. Rev. Lett.* **1992**, *68*, 3745 – 3748.
[39] A. Milner, A. Gerber, B. Groisman, M. Karpovsky, A. Gladkikh, *Phys. Rev. Lett.* **1996**, *76*, 475 – 478.
[40] J. Q. Wang, N. Dao, N. H. Kim, S. L. Whittenburg, *J. Appl. Phys.* **2004**, *95*, 6762.
[41] A. M. Mebed, J. M. Howe, *J. Appl. Phys.* **2006**, *100*, 074310.
[42] Y. Y. Chen, J. Ding, L. Si, W. Y. Cheung, S. P. Wong, I. H. Wilson, T. Suzuki, *Appl. Phys. A* **2001**, *73*, 103 – 106.
[43] C. L. Chien, J. Q. Xiao, J. S. Jiang, *J. Appl. Phys.* **1993**, *73*, 5309.
[44] V. Dupuis, J. Tuaillon, B. Prevel, A. Perez, P. Melinon, G. Guiraud, F. Parent, L. B. Steren, R. Morel, A. Barthelemy, A. Fert, S. Mangin, L. Thomas, W. Wernsdorfer, B. Barbara, *J. Magn. Magn. Mater.* **1997**, *165*, 42 – 45.
[45] M. Holdenried, B. Hackenbroich, H. Micklitz, *J. Magn. Magn. Mater.* **2001**, *231*, 13 – 19.
[46] S. Rubin, M. Holdenried, H. Micklitz, *J. Magn. Magn. Mater.* **1999**, *203*, 97 – 99.
[47] A. Weddemann, I. Ennen, A. Regtmeier, C. Albon, A. Wolff, K. Eckstädt, N. Mill, M. K.-H. Peter, J. Mattay, C. Plattner, N. Sewald, A. Hütten, *Beilstein J. Nanotechnol.* **2010**, *1*, 75 – 93.
[48] C. T. Black, C. B. Murray, R. L. Sandstrom, S. Sun, *Science* **2000**, *290*, 1131 – 1134.
[49] S. Miwa, M. Shiraishi, M. Mizuguchi, T. Shinjo, Y. Suzuki, *Jpn. J. Appl. Phys.* **2006**, *45*, L717 – L719.
[50] H. Kusai, S. Miwa, M. Mizuguchi, T. Shinjo, Y. Suzuki, M. Shiraishi, *Chem. Phys. Lett.* **2007**, *448*, 106.
[51] S. Tanabe, S. Miwa, M. Mizuguchi, T. Shinjo, Y. Suzuki, M. Shiraishi, *Appl. Phys. Lett.* **2007**, *91*, 063123.
[52] J. Dugay, R. P. Tan, A. Meffre, T. Blon, L.-M. Lacroix, J. Carrey, P. F. Fazzini, S. Lachaize, B. Chaudret, M. Respaud, *Nano Lett.* **2011**, *11*, 5128 – 5134.
[53] Y.-F. Chen, Y. Mei, R. Kaltofen, J. I. Mönch, J. Schumann, J. Freudenberger, H.-J. Klauß, O. G. Schmidt, *Adv. Mater.* **2008**, *20*, 3224.
[54] M. Melzer, D. Makarov, A. Calvimontes, D. Karnaushenko, S. Baunack, R. Kaltofen, Y. Mei, O. G. Schmidt, *Nano Lett.* **2011**, *11*, 2522.
[55] M. Melzer, D. Karnaushenko, D. Makarov, L. Baraban, A. Calvimontes, I. Monch, R. Kaltofen, Y. Mei, O. G. Schmidt, *RSC Adv.* **2012**, *2*, 2284.
[56] M. Melzer, G. Lin, D. Makarov, O. G. Schmidt, *Adv. Mater.* **2012**, *24*, 6468.

Received: February 14, 2013
Published online on April 8, 2013